

Indentation Fracture Toughness of Semiconducting Gallium Arsenide at Elevated Temperatures

Anthony Moulins¹, François Andrusyszyn¹, Roberto Dugnani^{2,a} and Ricardo J Zednik^{1,b}

¹École de Technologie Supérieure, Université du Québec, Montréal, Canada

²University of Houston – Clear Lake, Houston, Texas, USA

ABSTRACT

In this study, the temperature evolution of the fracture toughness in single-crystal gallium arsenide (GaAs) was investigated on the (001) plane using Vickers indentation. The highest temperature considered was 95 °C, corresponding to the typical maximum operating temperature of common GaAs semiconductor devices. Experimental results showed a decrease in hardness and an increase in toughness between 25 and 95 °C. GaAs cleavage planes were mostly composed of {110} and {100}, and predominantly aligned with the indenter's diagonal. Measured crack lengths were used to calculate the fracture toughness. Interestingly, the size of the primary cracks on {110} was found to be unaffected by temperature, while higher temperatures led to an increased formation of secondary {001} cracks and $\langle 110 \rangle$ slip. An Arrhenius-type model was found to describe the observed temperature dependence of the fracture toughness. This improved understanding of the mechanism underlying the mechanical properties of GaAs during fracture is particularly useful for the failure analysis of GaAs semiconductor devices, and highlights the importance of selecting appropriate crystallographic orientations if failure in GaAs devices is to be avoided.

Keywords: fracture toughness, Vickers indentation, gallium arsenide, hardness, temperature

^a Corresponding author: dugnani@uhcl.edu

^b Corresponding author: ricardo.zednik@etsmtl.ca

1. Introduction

Gallium arsenide (GaAs) based components are increasingly employed in high-performance semiconductor applications, including in the telecommunication, biomedical, and aerospace industries. GaAs single-crystals are widely used in microchips that operate at temperatures of around 20-75 °C [1]–[3]. Unfortunately, elevated operating temperatures result in large internal stresses that, in the worst case, result in catastrophic failure of the device [4]. Integrating GaAs components therefore often requires expensive cooling systems to reduce the risk of failure [5]. Despite GaAs's extensive utilization, the fracture behavior of GaAs remains poorly understood, particularly at typical operating temperatures, thereby complicating failure analysis. The limited literature available on the topic describes either the material's behavior at temperatures well-above customary application [6]–[8], or at room-temperature [9]–[13].

For brittle solids, indentation and hardness measurements are considered to be some of the simplest methods to studying the fracture behavior, as it does not require extensive testing and a large number of samples. In particular, Vickers indentation has been used to generate cracks in brittle materials that extend radially from the indentation. The fracture toughness of sapphire and spinel single crystals has been reported to correlate with the indentation crack length and with the diagonal impression of Vickers indenters [14]–[16]. Using dimensional analysis arguments, in the past, the isotropic K_{Ic} has been correlated to the ratio between the maximum contact pressure and the total crack length [14], [17]–[20].

Brookes et al. pointed out the anisotropy in the hardness of single crystals such as magnesium oxide, aluminium oxide, lithium fluoride, and calcium fluoride [21]. They proposed an analysis of the indentation process to correlate stress with the hardness, but the study was limited to the Knoop indenter. Lawn et al. proposed a model to describe the fracture toughness in long median/half penny cracks assuming quasi-static crack-growth in isotropic media (the “LEM model”) [16], [18]–[20]. Although the LEM model allows the estimation of the fracture toughness of isotropic materials, it imprecisely describes the contact stresses when applied to single crystals. Anstis et al. refined the LEM model by explicitly incorporating a residual stress intensity term into the strength formulation[19]. They noted that the ratio $P/c^{3/2}$ remained approximately invariant for both

sapphire and silicon single crystals where P was the maximum contact pressure and c the total median crack length. Unfortunately, the study did not provide a comprehensive description of the crack shape during the process of indentation, leading to large scatter in the predicted fracture toughness [14]. Niihara et al. extended the “Anstis-LEM” model to low crack-to-indent ratios and described the fracture toughness in the case of half-penny cracks (i.e. for $b/a > 2.5$) with shape factor $\zeta = 0.129$ [22]–[25]. For this scenario, Niihara et al. proposed:

$$K_{1c} = \frac{1}{\phi} \cdot \zeta H \sqrt{a} \cdot \left(\frac{E\phi}{H} \right)^{\frac{2}{5}} \left(\frac{b}{a} \right)^{-\frac{3}{2}} \quad (1.1)$$

In Eq. (1.1), $\phi = H/\sigma_y \cong 3$, with ϕ the plastic factor defined by the hardness H normalized by the yield strength σ_y , b and a are the total median crack length and the half diagonal length of the indenter impression, assuming half-penny cracks perpendicular to the plane of indentation and co-linear to the diagonal axis of the indenter, and E is the Young’s modulus. Regretfully, the material anisotropy inherent in single crystals is ignored in this formulation.

The elastic components are typically harmonized in the literature, and often no crystallographic reference is given with respect to the specimen/crystal orientation apart from the recent quantitative studies on GaAs [13]. The harmonization of GaAs’s mechanical properties combined with the plethora of the methods/models developed to estimate the fracture toughness from indentations have led to considerable scatter in the reported magnitudes of K_{1c} [9], [26]–[28]. Moreover, the addition of temperature further complicates the estimation of fracture strength in single crystal GaAs [8], [29], [30].

The goal of this study is therefore to advance our understanding of the fracture behavior in single crystal GaAs in the temperature range between 25 to 95 °C while considering crystal anisotropy. Specifically, this work focuses on the evaluation of the fracture toughness using a directional elastic modulus orthogonal to the crack propagation direction and it is based on a generalization of Niihara et al.’s model described by Eq. (1.1) and already applied to similar class of single crystals. Following this methodology, the fracture toughness was investigated with respect to the dominant fracture direction [110]. Finally, an Arrhenius-type equation was fitted to the fracture toughness of GaAs at various temperatures to estimate the activation energy required for crack propagation.

2. Methodology

The maximum temperature considered in the study (95 °C) was selected based on the operating temperature of common GaAs semiconductor devices [1]–[3].

2.1. Anisotropy of GaAs Single Crystals

In this work, the effect of the anisotropic elastic modulus on strain field induced during crack propagation was considered through Niihara et al.'s formulation (Eq. (1.1)). For any $\langle uvw \rangle$ crystallographic zone axis inside $\{001\}$, K_{1c} in Eq. (1.1) was adjusted by replacing the isotropic E by the corresponding $E_{\{001\}}^{\langle uvw \rangle}$ according to GaAs crystal/specimen orientation [31], [32]. The directional elastic modulus was obtained from the equation:

$$1/E_{\{hkl\}}^{\langle uvw \rangle} = S_{11} - 2(S_{11} - S_{12} - \frac{1}{2}S_{44})(m^2n^2 + m^2p^2 + n^2p^2) \quad (2.1)$$

where m , n and p are the direction cosines of the angle lying between the crystallographic direction $[hkl]$ and the following crystal axis X (100), Y (010) and Z (001) according to the specimen orientation. Combining Eq. (1.1) and (2.1), the (001) GaAs fracture toughness was estimated in terms of the indentation parameters and the directional elastic component:

$$K_{1c\{001\}}^{\langle 110 \rangle} = \zeta H^{\frac{3}{5}} \left(\frac{a^{\frac{2}{3}}}{\sqrt{b}} \right)^3 \phi^{-\frac{3}{5}} E_{\{001\}}^{\langle 110 \rangle - \frac{2}{5}} \quad (2.2)$$

where S_{ij} are the elastic coefficients from the reduced cubic compliance matrix in Voigt form [33], [34]. In GaAs, S_{11} , S_{12} and S_{44} are respectively $11.7 \cdot 10^{-12} Pa^{-1}$, $-3.7 \cdot 10^{-12} Pa^{-1}$ and $16.8 \cdot 10^{-12} Pa^{-1}$. The hardness-to-yield stress ratio, $\phi \cong 3$ has been used in various cubic crystals [23]–[25], [35] and was therefore also used for the study of GaAs. Optical measurements of the crack lengths were performed for each median cracks C1, C3, C5 and C7 after the sample had cooled to room temperature. The fracture toughness was estimated by averaging the results obtained for each indentation.

In this work, it was assumed that no phase transition in GaAs occurred and that the effects of diffusion were negligible in the temperature range studied. An Arrhenius formulation was used to

correlate the fracture toughness $K_{1c\{001\}}^{\langle 110 \rangle}$ to the temperature [9]–[11], [36] as a function of the activation energy $E_{a\langle 110 \rangle}$ needed to propagate $\langle 110 \rangle$ cracks:

$$K_{1c\{001\}}^{\langle 110 \rangle} / \kappa_{\{001\}}^{\langle 110 \rangle} = e^{-\frac{E_{a\langle 110 \rangle}}{k_B T}} \quad (2.3)$$

with $\kappa_{\{001\}}^{\langle 110 \rangle}$ a constant to be determined, $k_B \approx 1.38 \times 10^{-23} \text{ J} \cdot \text{K}^{-1}$ the Boltzmann constant, and T the temperature in Kelvin.

2.2. Materials and Testing Apparatus

An automated microhardness Clemex tester with a Vickers indenter was used by adapting the Standard Test Method for Vickers Indentation Hardness of Advanced Ceramics (2019) [37] as well as the Standard Test Method for Micro-indentation Hardness of Materials (2017) [38]. In this work, a custom Peltier thermoelectric heater with a PID controller was adapted directly onto the Clemex system to control the temperature during indentation. The temperature was measured at $\pm 1^\circ \text{C}$ via a thermocouple contacting the sample and relatively constant once the Peltier cell was calibrated.

Undoped (001) GaAs wafers $625 \pm 20 \text{ }\mu\text{m}$ thick with one side mirror polished were used for the indentation testing. The crystal specimens were aligned to $\langle 110 \rangle$ with the Vickers indenter, as shown in Figure 2–1. A dwell time of 10 seconds per indent was used and both indentation and crack lengths were recorded using a 3D laser confocal microscope OLS4100 (Olympus) with 405 nm incident wavelength radiation. The lateral resolution of the confocal microscope was 120 nm with a height resolution of 10 nm. Only large median cracks C1, C3, C5 and C7 (Figure 2–1) were considered in the fracture toughness model (i.e. $b/a > 2.5$).

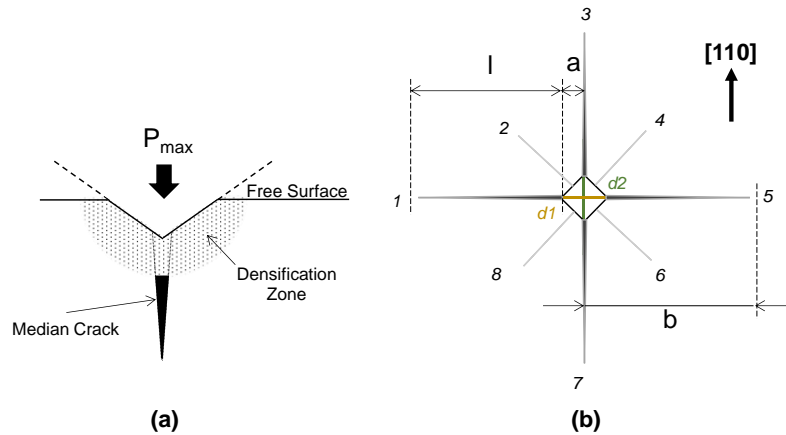


Figure 2-1 Representation of the GaAs indentation in the (001) plane with schematic view of (a) an elastic sharp contact pressure, P_{max} , and (b) top view of the indentation with the Vickers indenter aligned with $\langle 110 \rangle$ showing the crack nomenclature (C1 through C8)

Preliminary tests were carried out between 50 gf (~ 0.490 N) and 2 kgf (~ 19.6 N) to identify the load required to optimize the cracking and indentation quality. A load of 300 gf (~ 2.94 N) was found to lead to the best outcome in terms of crack size and number, as well as good surface quality without the formation of dust or fracture particles. A minimum distance of at least 4 times the averaged crack length was used between indentations. The automated microhardness tester operated four lines of seven indents for a total of 28 points per temperature. Indentations were carried out only with the sample's $\langle 110 \rangle$ aligned with the diagonal of the indenter.

3. Results And Discussion

For the range of temperature 25-95 °C, the total median crack length and b/a remained relatively constant at 55.3 ± 0.8 μm and 3.63 ± 0.14 , respectively, with b/a decreasing from 3.87 ± 0.05 to 3.34 ± 0.10 between 25-95 °C. The fracture toughness ranged from 0.49 (for C1-C5) and up to 0.58 $\text{MPa}\sqrt{\text{m}}$ (for C3-C7), in very good agreement with recent study supported by both experimental and simulations results [39] that found fracture toughness ranging from 0.50 ± 0.05 to 0.54 ± 0.04 $\text{MPa}\sqrt{\text{m}}$. GaAs hardness decreased by 23%. Figure 3-1 shows representative examples of Vickers indentations at 25 °C, 55 °C, and 95 °C.

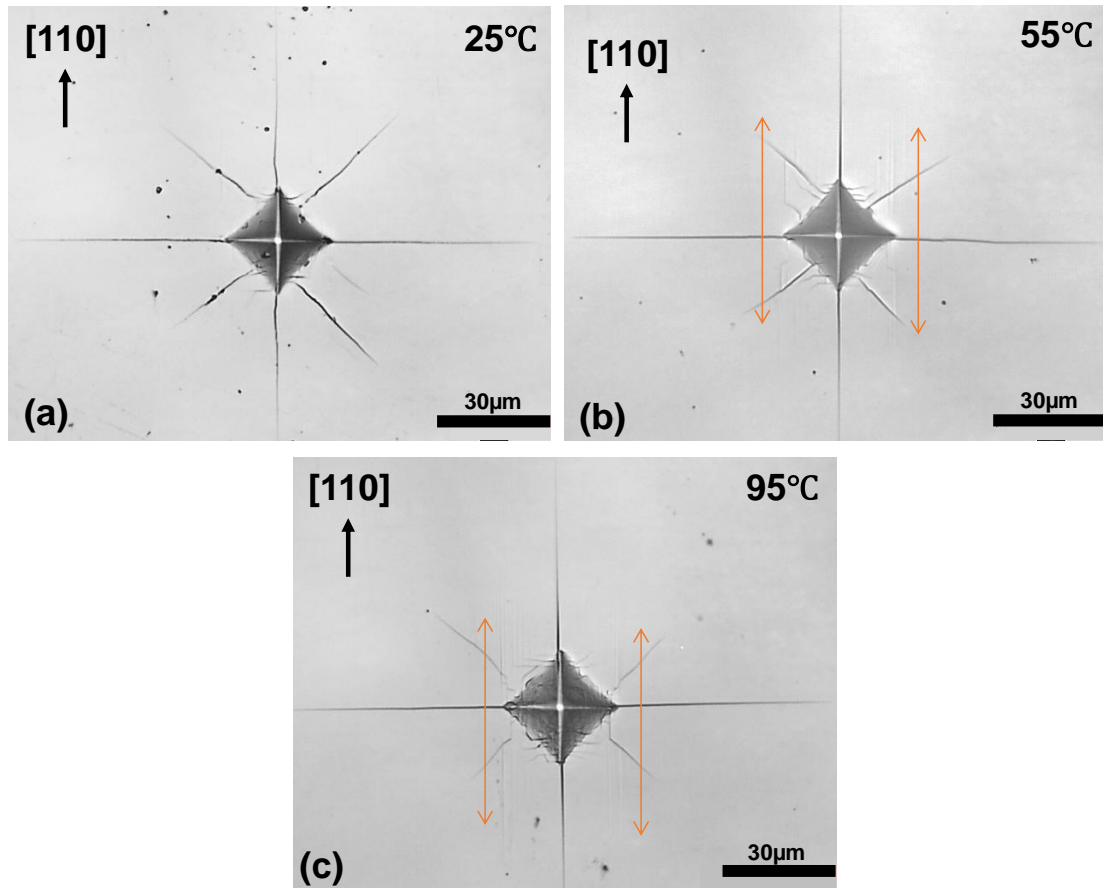


Figure 3–1 Vickers impression on GaAs at (a) 25 °C, (b) 55 °C, and (c) 95 °C at 300 gf. Note slip lines parallel to [110] present at higher temperatures.

The higher temperature indentations shown in Figure 3–1 (b) and (c) show the formation of slip lines (orange arrows) aligned along [110]. The activation of slip at higher temperature may occur due to dislocation migration, although further study is necessary to why they preferentially align with [110]. Moreover, around 55 to 65 °C, a decrease of the secondary (lateral C2-C4-C6-C8) cracks was observed.

The fracture toughness for the four dominant cracks C1, C3, C5, and C7 was estimated using Eq. (2.2) at various temperatures. The results are presented in Figure 3–2 with cracks identified according to Figure 2–1. The primary cracks C1 and C5 (aligned with the indenter diagonal) are comparable in length, with no significant change between 25-95 °C. This contrasts with the cracks C3 and C7 running along [110] that exhibited a more marked temperature dependency. This is consistent with the appearance of slip lines along [110], suggesting that this direction dominates the toughening mechanism in GaAs.

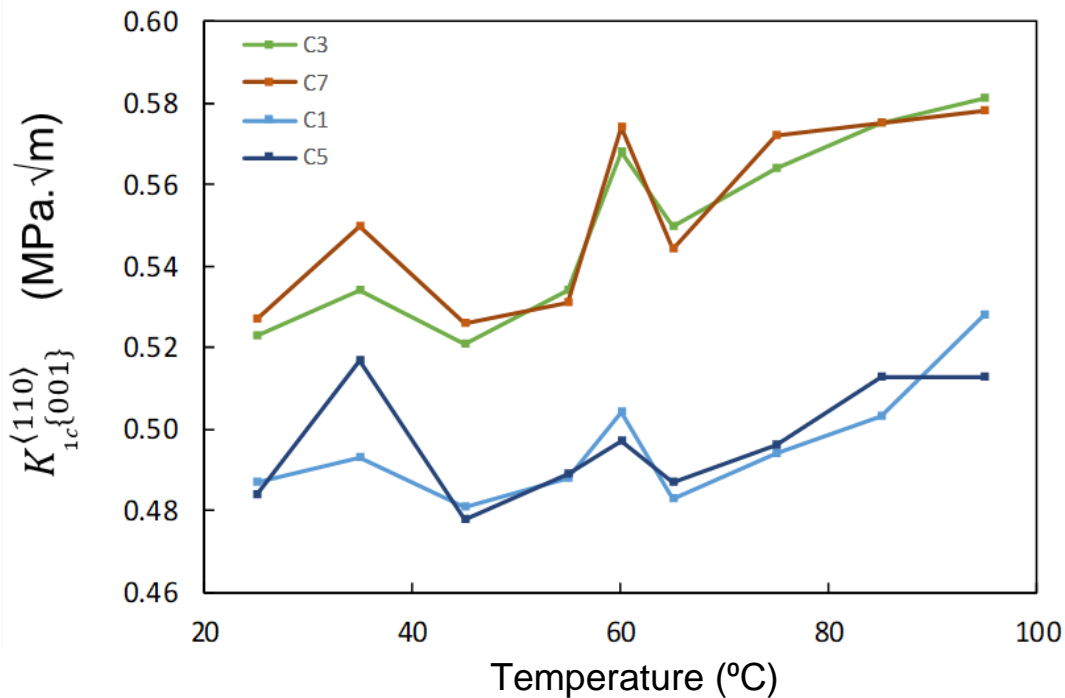


Figure 3–2 Evaluation of [110] fracture toughness of cracks C1, C3, C5, and C7 in GaAs as a function of temperature.

An overall “average” fracture toughness was calculated by averaging the fracture toughnesses across the observed cracks. The averaged fracture toughness increased from 25 °C with $\overline{K_{1c\{001\}}^{[110]}} = 0.51 \pm 0.02 \text{ MPa}\sqrt{\text{m}}$ up to $\overline{K_{1c\{001\}}^{[110]}} = 0.55 \pm 0.03 \text{ MPa}\sqrt{\text{m}}$ at 95 °C, as shown in Figure 3–3. Simultaneously, the measured hardness of GaAs decreases from $H_{25^\circ\text{C}} = 674 \pm 24 \text{ HV}$ to $H_{95^\circ\text{C}} = 524 \pm 9.8 \text{ HV}$; this corresponds to an approximate expected GaAs yield stress range of $\sigma_{Y(25^\circ\text{C})} = 2.2 \pm 0.1 \text{ GPa}$ to $\sigma_{Y(95^\circ\text{C})} = 1.7 \pm 0.1 \text{ GPa}$.

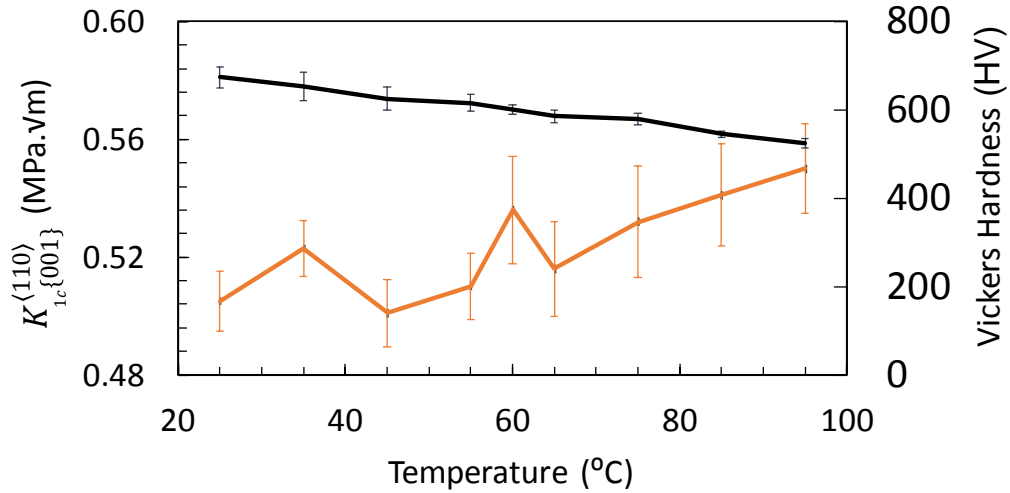


Figure 3-3 Evolution of GaAs Vickers hardness (black line, right axis) and fracture toughness K_{Ic} (orange line, left axis) for 25-95°C

Figure 3-4 shows the average fracture toughness versus temperature and the fit to an Arrhenius model provided by Equation (2.3). The fit allowed us to extract the toughness parameter $\kappa_{\{001\}}^{(110)} = 0.81 \pm 0.08 \text{ MPa}\sqrt{\text{m}}$ and the activation energy $E_a = 2.1 \pm 0.4 \cdot 10^{-21} \text{ J}$, consistent with dislocation movement as the primary toughening mechanism.

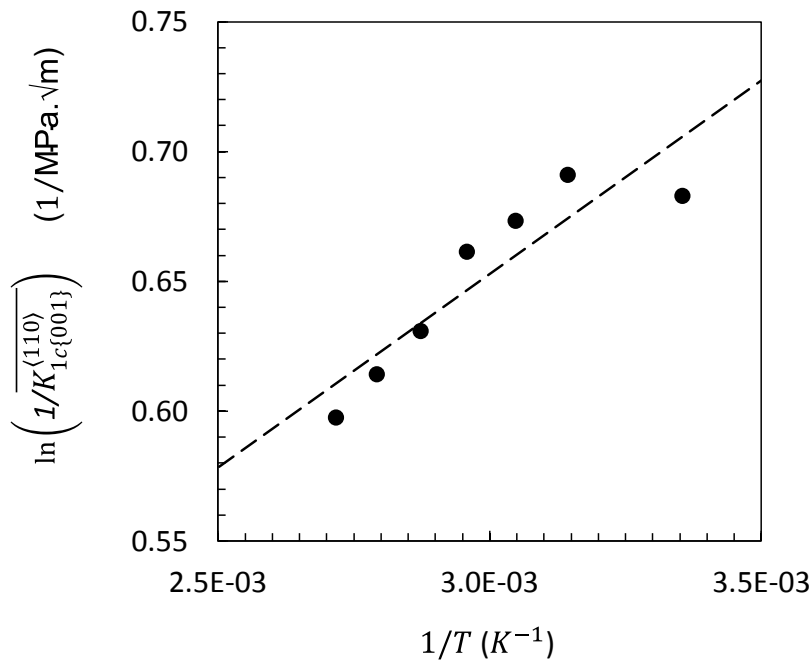


Figure 3-4 Arrhenius model fitted to experimental GaAs fracture toughness

4. Conclusions

This study investigated the fracture toughness of (001) GaAs single crystals in the temperature range 25-95 °C. The appearance of slip lines along $\langle 110 \rangle$ occurred at higher temperatures, suggesting this as a likely toughening mechanism. A 23% decrease in Vickers hardness between 25-95 °C with $H_{(001)}$ ranging from $H_{25^\circ\text{C}} = 674 \pm 24$ HV to $H_{95^\circ\text{C}} = 524 \pm 9.8$ HV correlated with an increase in toughness ranging from 0.49 (for C1-C5) and up to 0.58 $\text{MPa}\sqrt{\text{m}}$ (for C3-C7). The generalized toughness model presented in this work addressed the anisotropy of GaAs and toughness obtained was in very good agreement with recent literature. Moreover, the toughness formulation helped develop a simplified Arrhenius model to describe the effect of temperature. An activation energy of $E_a = 2.1 \pm 0.4 \cdot 10^{-21}$ J was found for crack propagation. The proposed model displayed a nearly linear relationship between temperature and toughness in the temperature range 25-95 °C. Although the assumptions made along with the model proposed in this work do not apply to very high temperatures, i.e., where diffusion becomes significant and/or phase transformations occur, they were valid for the temperature range considered and the proposed model described the toughness behavior of GaAs adequately. This improved understanding of the mechanical behavior of this important semiconductor material is useful for analyzing failed GaAs devices that commonly operate in this temperature range. The results also provide a framework for aligning semiconductor device architecture with the appropriate crystallographic directions to ensure improved resistance to mechanical failure. In addition, the Vickers indentation approach used to understand the temperature-dependent toughness of GaAs could be further generalized to help improve our understanding of other technologically important crystals at elevated temperatures.

Acknowledgments

The authors would like to thank Professor Philippe Bocher for his valuable advice and access to the Clemex system as well as Dr. Yasser Zedan for technical assistance and Mr. Michel Drouin, ing., for his help with the realization of the micro-heating system.

Funding Sources

The authors also wish to acknowledge the Natural Sciences and Engineering Research Council of Canada (NSERC) Discovery Grant RGPIN-2015-04185, MITACS Globalink Grant IT09006, the École de Technologie Supérieure (ÉTS) Programme Impulsion, and ÉTS Fonds pour la collaboration international de recherche for funding.

References

- [1] L. Li, R. Coccioli, K. Nary, and P. Canfield, “Multi-scale thermal analysis of GaAs RF device,” in *Annual IEEE Semiconductor Thermal Measurement and Management Symposium*, 2005, pp. 259–263.
- [2] V. Milutinovic, D. Fura, and H. Walter, “An Introduction to GaAs Microprocessor Architecture for VLSI,” *Computer (Long. Beach. Calif.)*, vol. 19, no. 3, pp. 30–42, 1986.
- [3] V. Milutinovic, “Microprocessor architecture and design for GaAs technology,” *Microelectronics J.*, vol. 19, no. 4, pp. 51–55, 1988.
- [4] R. Dugnani and R. J. Zednik, “Flexural strength by fractography in modern brittle materials,” *J. Am. Ceram. Soc.*, vol. 96, no. 12, pp. 3908–3914, 2013.
- [5] H. F. Hamann *et al.*, “Hotspot-limited microprocessors: Direct temperature and power distribution measurements,” *IEEE J. Solid-State Circuits*, vol. 42, no. 1, pp. 56–64, Jan. 2007.
- [6] P. Borvin, J. Rabier, H. Garem, and P. Borvin, “Plastic deformation of GaAs single crystals as a function of electronic doping I: Medium temperatures (150–650°C),” *Philos. Mag. A Phys. Condens. Matter, Struct. Defects Mech. Prop.*, vol. 61, no. 4, pp. 619–645, 1990.
- [7] D. Laister and G. M. Jenkins, “Deformation of single crystals of gallium arsenide,” *J. Mater. Sci.*, vol. 8, no. 9, pp. 1218–1232, Sep. 1973.
- [8] V. Swaminathan and S. M. Copley, “Temperature and Orientation Dependence of Plastic Deformation in GaAs Single Crystals Doped with Si, Cr, or Zn,” *J. Am. Ceram. Soc.*, vol. 58, no. 11–12, pp. 482–485, 1975.
- [9] J. S. Blakemore, “Semiconducting and other major properties of GaAs,” *J. Appl. Phys.*, vol. 53, no. 10, p. R123, 1982.
- [10] C. Pouvreau *et al.*, “Nanoindentation cracking in gallium arsenide: Part II. TEM

- investigation,” *J. Mater. Res.*, vol. 28, no. 20, pp. 2799–2809, 2013.
- [11] K. Maeda, H. Nishioka, N. Narita, and S. Fujita, “Brittle-to-ductile transition studied by constant-rate indentation cracking,” *Mater. Sci. Eng. A*, vol. 176, no. 1–2, pp. 121–126, Mar. 1994.
- [12] S. Fujita, K. Maeda, and S. Hyodo, “Dislocation-mobility-controlled cracking in gaas caused by constantrate indentation,” *Philos. Mag. A Phys. Condens. Matter, Struct. Defects Mech. Prop.*, vol. 65, no. 1, pp. 131–147, 1992.
- [13] A. Moulins, R. Dugnani, and R. J. Zednik, “Fracture surface analysis and quantitative characterization of gallium arsenide III-V semiconductors using fractography,” *Eng. Fail. Anal.*, vol. 123, p. 105313, May 2021.
- [14] J. H. Lee, Y. F. Gao, K. E. Johanns, and G. M. Pharr, “Cohesive interface simulations of indentation cracking as a fracture toughness measurement method for brittle materials,” *Acta Mater.*, vol. 60, no. 15, pp. 5448–5467, Sep. 2012.
- [15] A. G. Evans and E. A. Charles, “Fracture Toughness Determinations by Indentation,” *J. Am. Ceram. Soc.*, vol. 59, no. 7–8, pp. 371–372, Jul. 1976.
- [16] B. R. Lawn and R. Wilshaw, “Indentation fracture: principles and applications,” *Journal of Materials Science*, vol. 10, no. 6. Kluwer Academic Publishers, pp. 1049–1081, Jun-1975.
- [17] M. Sebastiani, K. E. Johanns, E. G. Herbert, and G. M. Pharr, “Measurement of fracture toughness by nanoindentation methods: Recent advances and future challenges,” *Current Opinion in Solid State and Materials Science*, vol. 19, no. 6. Elsevier Ltd, pp. 324–333, 01-Dec-2015.
- [18] B. R. Lawn, A. G. Evans, and D. B. Marshall, “Elastic/Plastic Indentation Damage in Ceramics: The Median/Radial Crack System,” *J. Am. Ceram. Soc.*, vol. 63, no. 9–10, pp. 574–581, 1980.
- [19] G. R. Anstis, P. Chantikul, B. R. Lawn, and D. B. Marshall, “A Critical Evaluation of Indentation Techniques for Measuring Fracture Toughness: I, Direct Crack Measurements,” *J. Am. Ceram. Soc.*, vol. 64, no. 9, pp. 533–538, 1981.
- [20] G. R. Anstis, P. Chantikul, B. R. Lawn, and D. B. Marshall, “A Critical Evaluation of Indentation Techniques for Measuring Fracture Toughness: II, Strength Method,” *J. Am. Ceram. Soc.*, vol. 64, no. 9, pp. 533–538, 1981.
- [21] C. A. Brookes, J. B. O’Neill, and B. A. W. Redfern, “Anisotropy in the Hardness of Single

- Crystals,” *Proc. R. Soc. A Math. Phys. Eng. Sci.*, vol. 322, no. 1548, pp. 73–88, Mar. 1971.
- [22] K. Niihara, “A fracture mechanics analysis of indentation-induced Palmqvist crack in ceramics,” *J. Mater. Sci. Lett.*, vol. 2, no. 5, pp. 221–223, 1983.
- [23] H. Li and F. Ebrahimi, “Synthesis and characterization of electrodeposited nanocrystalline nickel-iron alloys,” *Mater. Sci. Eng. A.*, vol. 347, no. 1–2, pp. 93–101, Apr. 2003.
- [24] F. Ebrahimi and L. Kalwani, “Fracture anisotropy in silicon single crystal,” *Mater. Sci. Eng. A*, vol. 268, no. 1–2, pp. 116–126, Aug. 1999.
- [25] M. Tanaka, K. Higashida, H. Nakashima, H. Takagi, and M. Fujiwara, “Fracture toughness evaluated by indentation methods and its relation to surface energy in silicon single crystals,” *Mater. Trans.*, vol. 44, no. 4, pp. 681–684, 2003.
- [26] K. Yasutake, Y. Konishi, K. Adachi, K. Yoshii, M. Umeno, and H. Kawabe, “Fracture of GaAs Wafers,” *Jpn. J. Appl. Phys.*, vol. 27, no. 12R, pp. 2238–2246, 1988.
- [27] G. Michot, A. George, A. Chabli-Brenac, and E. Molva, “Fracture toughness of pure and In-doped GaAs,” *Scr. Metall.*, vol. 22, no. 7, pp. 1043–1048, Jan. 1988.
- [28] S. G. Roberts, P. D. Warren, and P. B. Hirsch, “Knoop hardness anisotropy on {001} faces of germanium and gallium arsenide,” *J. Mater. Res.*, vol. 1, no. 1, pp. 162–176, 1986.
- [29] S. Wang and P. Pirouz, “Mechanical properties of undoped GaAs. III: Indentation experiments,” *Acta Mater.*, vol. 55, no. 16, pp. 5526–5537, 2007.
- [30] C. Y. Lou and G. A. Somorjai, “Studies of the vaporization mechanism of gallium arsenide single crystals,” *J. Chem. Phys.*, vol. 55, no. 9, pp. 4554–4565, Nov. 1971.
- [31] J. B. Wachtman, “Determination of Elastic Constants Required for Application of Fracture Mechanics to Ceramics,” in *Concepts, Flaws, and Fractography*, Springer US, 1974, pp. 49–68.
- [32] A. Kelly and N. H. Macmillan, *Strong Solids*, 3rd ed. Walton Street, Oxford: Oxford Clarendon Press, 1986.
- [33] R. W. Margevicius and R. Gumbsch, “Influence of crack propagation direction on (110) fracture toughness of gallium arsenide,” *Philos. Mag. A Phys. Condens. Matter, Struct. Defects Mech. Prop.*, vol. 78, no. 3, pp. 567–581, 1998.
- [34] K. Hjort, J. Soderkvist, and J. A. Schweitz, “Gallium arsenide as a mechanical material,” *J. Micromechanics Microengineering*, vol. 4, no. 1, pp. 1–13, 1994.
- [35] D. Tabor, *The hardness of metals*, Clarendon. Oxford: Oxford university press, 1951.

- [36] S. Fujita, K. Maeda, and S. Hyodo, “Dislocation-mobility-controlled cracking in GaAs caused by constant-rate indentation,” *Philos. Mag. A Phys. Condens. Matter, Struct. Defects Mech. Prop.*, vol. 65, no. 1, pp. 131–147, 1992.
- [37] ASTM C1327-15, “Standard Test Method for Vickers Indentation Hardness of Advanced Ceramics,” *ASTM Int.*, pp. 1–10, 2019.
- [38] ASTM E384-99, “Standard Test Method for Microindentation Hardness of Materials,” *ASTM Int.*, pp. 1–40, 2017.
- [39] J. Ast, J. J. Schwiedrzik, N. Rohbeck, X. Maeder, and J. Michler, “Novel micro-scale specimens for mode-dependent fracture testing of brittle materials: A case study on GaAs single crystals,” *Mater. Des.*, vol. 193, p. 108765, Aug. 2020.